Reaction mechanism of the binuclear zinc enzyme glyoxalase II – A theoretical study

ARTICLE *in* JOURNAL OF INORGANIC BIOCHEMISTRY · NOVEMBER 2008

Impact Factor: 3.44 · DOI: 10.1016/j.jinorgbio.2008.10.016 · Source: PubMed

3 AUTHORS, INCLUDING:

Wei-Hai Fang
Beijing Normal University
234 PUBLICATIONS **4,486** CITATIONS

SEE PROFILE

Journal of Inorganic Biochemistry 103 (2009) 274–281

Contents lists available at ScienceDirect

Journal of Inorganic Biochemistry

journal homepage: www.elsevier.com/locate/jinorgbio

Reaction mechanism of the binuclear zinc enzyme glyoxalase II – A theoretical study

Shi-Lu Chen [a,b], Wei-Hai Fang [b,*], Fahmi Himo [a,*]

[a] Department of Theoretical Chemistry, School of Biotechnology, Royal Institute of Technology, SE-10691 Stockholm, Sweden
[b] College of Chemistry, Beijing Normal University, Beijing 100875, PR China

ARTICLE INFO

Article history:
Received 4 August 2008
Received in revised form 14 October 2008
Accepted 20 October 2008
Available online 31 October 2008

Keywords:
Glyoxalase II
Binuclear zinc enzymes
Density functional theory
Reaction mechanism

ABSTRACT

The glyoxalase system catalyzes the conversion of toxic methylglyoxal to nontoxic D-lactic acid using glutathione (GSH) as a coenzyme. Glyoxalase II (GlxII) is a binuclear Zn enzyme that catalyzes the second step of this conversion, namely the hydrolysis of S-D-lactoylglutathione, which is the product of the Glyoxalase I (GlxI) reaction. In this paper we use density functional theory method to investigate the reaction mechanism of GlxII. A model of the active site is constructed on the basis of the X-ray crystal structure of the native enzyme. Stationary points along the reaction pathway are optimized and the potential energy surface for the reaction is calculated. The calculations give strong support to the previously proposed mechanism. It is found that the bridging hydroxide is capable of performing nucleophilic attack at the substrate carbonyl to form a tetrahedral intermediate. This step is followed by a proton transfer from the bridging oxygen to Asp58 and finally C–S bond cleavage. The roles of the two zinc ions in the reaction mechanism are analyzed. Zn2 is found to stabilize the charge of tetrahedral intermediate thereby lowering the barrier for the nucleophilic attack, while Zn1 stabilizes the charge of the thiolate product, thereby facilitating the C–S bond cleavage. Finally, the energies involved in the product release and active-site regeneration are estimated and a new possible mechanism is suggested.

1. Introduction

The glyoxalase system, composed of two distinct enzymes (glyoxalase I and II), catalyzes the conversion of toxic 2-oxoaldehydes to the corresponding 2-hydroxycarboxylic acids using glutathione (GSH) as a cofactor [1–3]. In particular, the system can detoxify methylglyoxal, a byproduct of carbohydrate and lipid metabolism [4,5], which can produce toxic effects by reacting with RNA, DNA, and proteins [4,6,7]. Glyoxalase I (GlxI) converts thiohemiacetal (formed from methylglyoxal and glutathione) to S-D-lactoylglutathione, while Glyoxalase II (GlxII) takes the latter as a substrate and catalyzes its hydrolysis to yield D-lactic acid and GSH (Scheme 1). S-D-lactoylglutathione is also known to exhibit cytotoxic effects through the inhibition of DNA synthesis [4]. GlxI and GlxII are thus thought to play an indispensable role in chemical detoxification [4,8]. In addition, the glyoxalase system has been suggested as a target in the design of anti-cancer and anti-protozoal drugs [5,9–14].

While GlxI is a mononuclear zinc enzyme [15–19], GlxII utilizes a binuclear metallosite to catalyze its reaction. It has a turnover number (k_{cat}) of $2.8 \times 10^2\ s^{-1}$ and a k_{cat}/K_m value of $8.8 \times 10^5\ M^{-1}\ s^{-1}$ for S-D-lactoylglutathione substrate [20]. GlxII generally requires two divalent zinc ions for catalytic activity [21–23]. However, this is not an absolute requirement. GlxII from *Arabidopsis thaliana* [24–27] and *Salmonella typhimurium* [28], for example, show metal-binding flexibility in that a variety of bimetallic sites, with iron, manganese, or zinc embedded, have been characterized.

Several X-ray crystal structures of GlxII have been determined [23,28,29], including *human* GlxII (PDB entry 1QH3) and its complex with a glutathione thioester substrate analogue (PDB entry 1QH5) [23]. It was shown that GlxII belongs to the metallo-β-lactamase superfamily of proteins, in which a zinc-binding motif is conserved [30]. The active site of GlxII contains a binuclear zinc center that is bridged by one oxygen of the Asp134 and an oxygen species (see Fig. 1), which has been suggested to be a hydroxide (μ-OH^-) [23]. A bridging hydroxide has been implicated in several other binuclear zinc enzymes, including metallo-β-lactamase from *Bacteroides fragilis* [31,32], phosphotriesterase (PTE) [33–35], and aminopeptidase from *Aeromonas proteolytica* (AAP) [36,37]. The two zinc ions are bound to the protein via the side chains of His54, His56, His110, Asp58, His59, and His173. Asp58 forms a hydrogen bond to the bridging hydroxide, suggesting that it plays a role in orienting the hydroxide for attacking on the substrate [24].

* Corresponding authors. Fax: +86 10 58802075 (W.H. Fang), +46 8 55378590 (F. Himo).
E-mail addresses: fangwh@bnu.edu.cn (W.-H. Fang), himo@theochem.kth.se (F. Himo).

0162-0134/$ - see front matter © 2008 Elsevier Inc. All rights reserved.
doi:10.1016/j.jinorgbio.2008.10.016

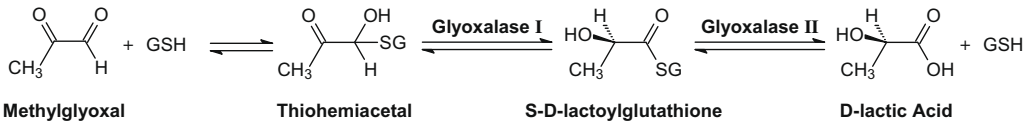

Scheme 1. Reactions catalyzed by the glyoxalase system.

Based on the crystal structures and other kinetic, spectroscopic, and mutational studies, the following reaction mechanism (presented in Scheme 2) has been proposed for GlxII [23,24]. The S-D-lactoylglutathione substrate docks first onto the active site, mainly by the binding of the glutathione moiety to the protein, particularly via its glycine and cysteine residues. The carbonyl oxygen of lactoyl group (O_C) is proposed to coordinate to Zn2 ion [23]. The bridging hydroxide (μ-OH^-) then performs a nucleophilic attack at the carbonyl carbon of lactoyl group (C_C) leading to the formation of a tetrahedral *gem*-diolate intermediate [23,24]. Zn2 stabilizes this negatively charged intermediate, and no protein residues near to the O_C atom were found to provide additional stabilization [23]. Next, the C_C–S bond of substrate breaks with help of the Zn1 ion [24], resulting in a D-lactic acid and an unprotonated glutathione (GS^-). To complete the reaction, the GS^- group is protonated by a water molecule and the products are released from the active site to regenerate the enzyme. Exactly how these steps occur is, however, still unclear.

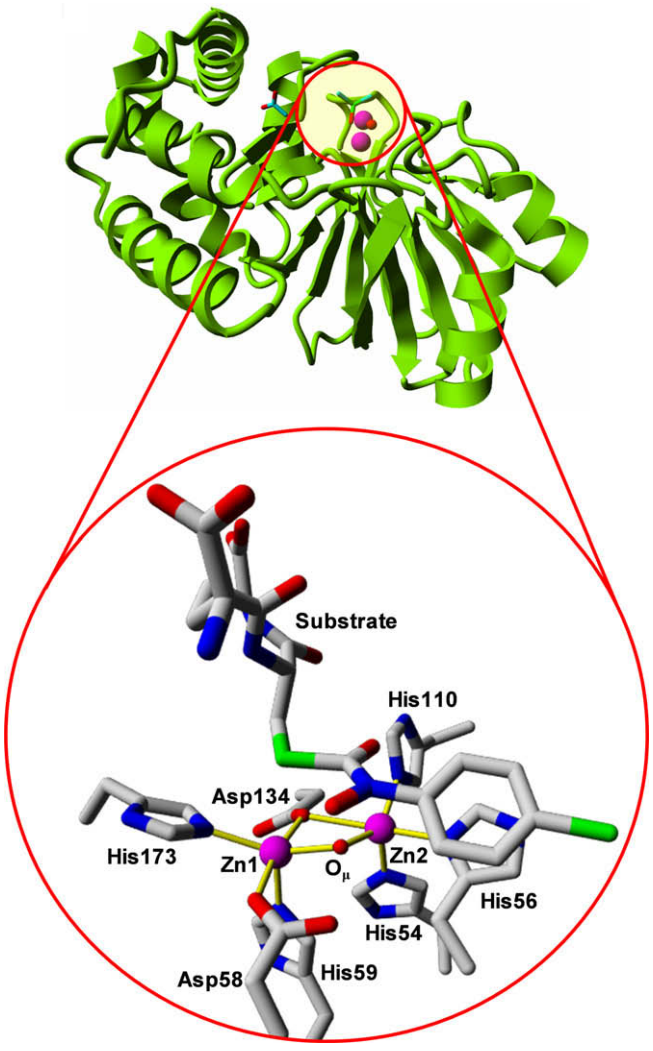

Fig. 1. Overall structure of *human* GlxII and close-up view of the active site. Coordinates from PDB entry 1QH5 were used to generate the figures [23]. The enzyme is in complex with a slow substrate, S-(N-hydroxy-N-bromophenylcarbamoyl) glutathione.

In recent years, quantum chemical modeling of enzyme active sites has proved to be a very fruitful approach to explore reaction mechanisms and to provide insight into various aspects of catalysis [38–42]. The workhorse of this approach has been density functional theory (DFT), and in particular the hybrid B3LYP functional [43–45]. In the present work, we use this method to investigate the reaction mechanism of GlxII. With a model of the active site constructed on the basis of the crystal structure (PDB entry 1QH5) [23], B3LYP is employed to calculate a potential energy surface for the reaction and to provide characterization of the transition states and intermediates involved. We have previously used the same approach to study the reaction mechanisms of a number of related di-zinc enzymes, such as phosphotriesterase (PTE) [34,35], aminopeptidase from *A. proteolytica* (AAP) [37], and dihydroorotase (DHO) [46].

2. Computational methods

All calculations were performed using the hybrid density functional theory functional B3LYP [43–45]. Geometry optimizations were carried out with the 6-31G(d,p) basis set for the C, H, O, N, and S elements, and the effective core potential LANL2DZ basis set for Zn. Based on these optimized geometries, more accurate energies were obtained by performing single point calculations with the larger basis set 6-311+G(2d,2p) for all elements. To estimate the effects of the missing protein environment on the calculated energies, solvation effects were calculated at the same theory level as the optimizations by performing single point calculations on the optimized structures using the CPCM method [47–50]. The dielectric constant (ε) was chosen to be 4, which is a standard value that has been used in many previous studies [35,51]. Frequency calculations were performed at the same theory level as the optimizations to obtain zero-point energies (ZPE) and to confirm the nature of the stationary points. This implies no negative eigenvalues for minima and only one negative eigenvalue for transition states. As will be discussed below, some atoms were kept fixed to their X-ray crystal positions. This procedure gives rise to a few small imaginary frequencies, typically on the order of $20i$ cm^{-1}. These frequencies do not contribute significantly to the ZPE and should thus not affect the accuracy of the energies. However, they render the evaluation of the entropy effects unreliable. Therefore, entropy was not considered in the present study.

The energies reported here are corrected for both solvation and zero-point vibrational effects. All calculations were performed using the Gaussian03 program package [52].

3. Results and discussion

3.1. Active-site model

A model of the active site of GlxII was constructed on the basis of the crystal structure of the wild-type *human* GlxII in complex with a slow substrate, S-(N-hydroxy-N-bromophenylcarbamoyl)

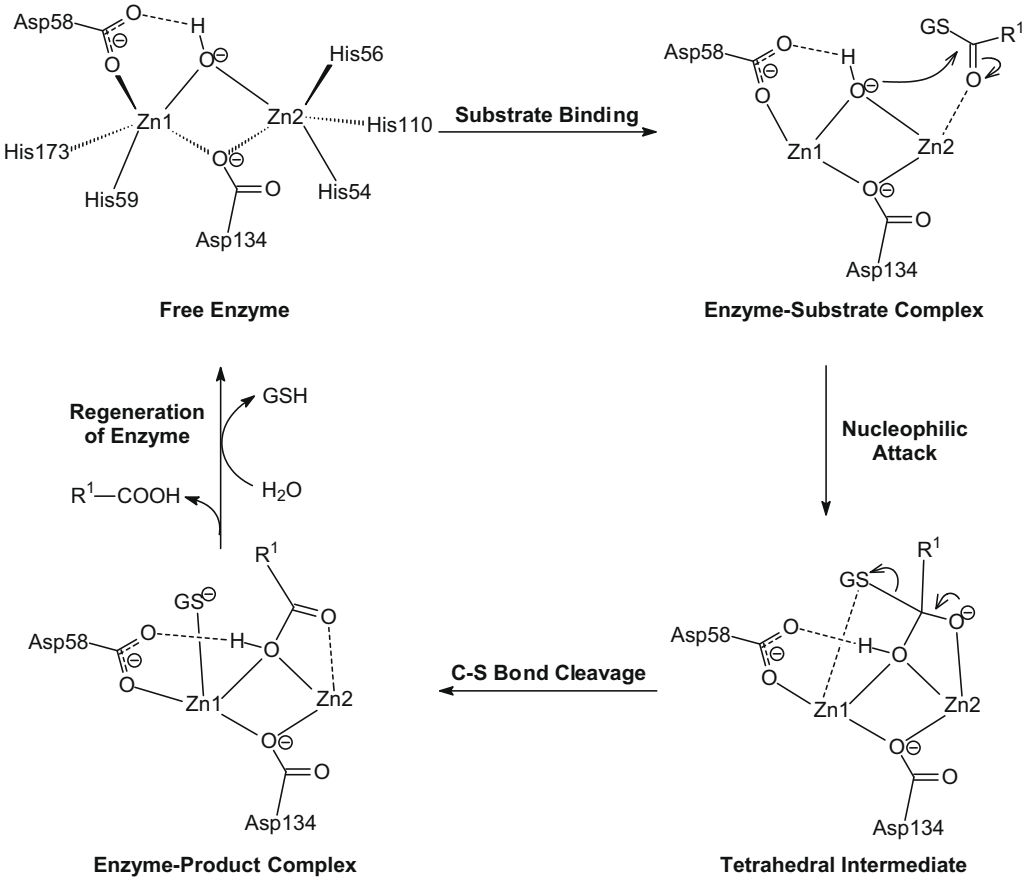

Scheme 2. Proposed reaction mechanism for GlxII.

glutathione (PDB entry 1QH5) [23]. The model was cut out manually from the PDB structure. It contains the two zinc ions along with their first-shell ligands His54, His56, His110, Asp58, His59, His173, and the bridging Asp134 and hydroxide (μ-OH^-). The ligands were truncated such that histidines were represented by imidazoles and aspartates and glutamates by acetates. Hydrogen atoms were added manually. The atoms where the truncation was done were kept fixed during the geometry optimizations to preserve the spatial arrangement of the residues. These centers are indicated by arrows in the figures below. In a previous study on the related phosphotriesterase enzyme, it was shown that this procedure is quite sound as the effects on the energy profile are not very large [35]. As a model substrate, we chose a small thioester formed from lactic acid and methylthiol (see Fig. 2), which serves the purpose of this study. The substrate was placed manually close to the model of the dinuclear Zn site. The total number of atoms in the model is 78 and the total charge is +1.

The optimized structure of the GlxII active site with the model substrate bound, corresponding to the Michaelis complex and referred to as *React* hereafter, is displayed in Fig. 2. The overall geometric parameters obtained from the geometry optimization agree quite well with the X-ray structure. For example, the bond distances of the bridging hydroxide to the two zinc ions are calculated to be 1.99 and 1.95 Å, to be compared to the crystallographic distances of 2.03 and 1.99 Å [23]. The computed Zn–Zn distance of 3.29 Å is also in very good agreement with the crystallographic distance of 3.34 Å [23].

It is interesting to note that the substrate does not coordinate to any of the zinc ions in the Michaelis complex. Instead, the hydroxyl group forms a hydrogen bond to the Asp58 residue. This hydrogen bond could be an artifact of the relative smallness of the model. In the real enzyme, one can envision that the extended substrate binds to the enzyme through other groups not present in the mod-

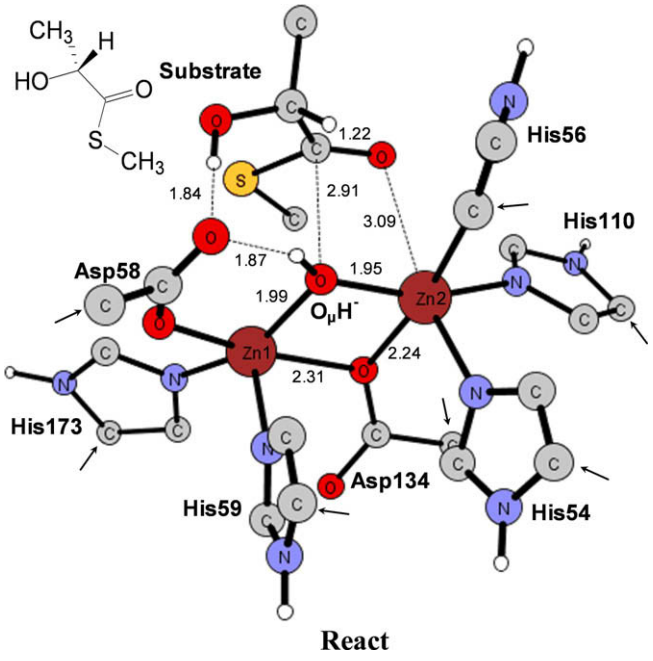

Fig. 2. Optimized structure of the GlxII active site with the model substrate bound. For clarity, some hydrogen atoms are omitted, which is also applied to other figures below. Arrows indicate the atoms that are fixed to their X-ray positions. Inserted is the model substrate used in the calculations. All distances are given in angstrom (Å).

els of the active site or the substrate, such as its glycine and cysteine parts. However, these interactions would be constant and do not change during the reactions. They contribute thus only to the binding, which makes the use of the current model safe for the purpose of studying the chemical steps of the reaction of the enzyme.

3.2. Nucleophilic attack

The first step of the proposed mechanism is the nucleophilic attack of the bridging oxygen (O_μ) on the carbonyl carbon (C_C) of substrate [23,24]. In *React*, the distance between these two atoms is 2.91 Å (Fig. 2). We have optimized the transition state (called *TS1*) and the resulting tetrahedral intermediate (*Inter1*) for this nucleophilic attack. The structures are shown in Fig. 3. We observe that the nucleophilic attack takes place directly from the bridging position. The nature of *TS1* was confirmed to be a first-order saddle point with an imaginary frequency of 204*i* cm^{-1}, which correlates with a vibrational mode of the O_μ–C_C bond formation. The energy barrier is calculated to be 18.2 kcal/mol. Upon addition of surrounding solvation in the form of CPCM, the barrier increases slightly to 19.2 kcal/mol (i.e. the solvation energy of *React* is 1.0 kcal/mol larger than that of *TS1*). The intermediate is calculated to be 17.1 kcal/mol higher than *React* (19.1 kcal/mol including solvation).

It is interesting to follow some geometrical changes that take place in going from *React* to *Inter1*, via *TS1* (see Figs. 2 and 3), as

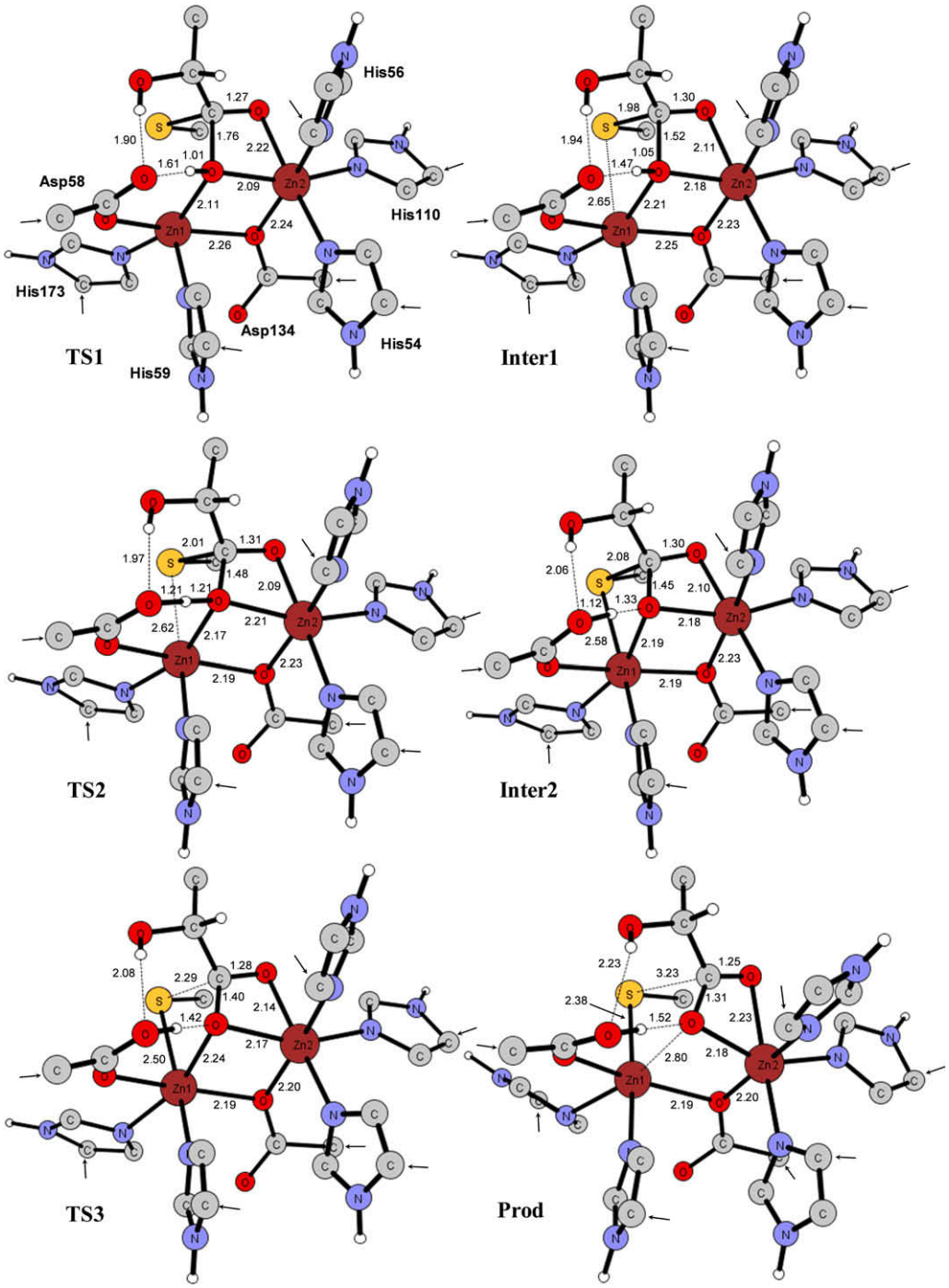

Fig. 3. Optimized structures of transition states and intermediates along the reaction pathway.

these can provide important chemical information. The critical O_μ–C_C distance is 1.76 Å at *TS1* and becomes 1.52 Å at *Inter1*. The bridging O_μ remains bridging throughout the reaction step, with O_μ–Zn bond distances of 2.21 Å and 2.18 Å in *Inter1*. The substrate carbonyl double bond (O_C–C_C) is elongated from 1.22 Å in *React* to 1.30 Å in *Inter1* (1.27 Å at *TS1*). As a result, the developing oxyanion at the O_C atom coordinates to the Zn2 ion (2.22 Å at *TS1* and 2.11 Å at *Inter1*). This demonstrates that Zn2 provides catalytic power by stabilizing the emerging negative charge at the O_C atom of the tetrahedral intermediate. Similar function for one of the zinc ions has been established also for other binuclear zinc enzymes, such as phosphotriesterase [34], aminopeptidase from *A. proteolytica* [37], and dihydroorotase [46]. Another interesting observation here is that since both O_μ and Asp134 remain bridging, Zn2 becomes hexa-coordinated. This is quite unusual for zinc enzymes, and is probably related to the fact that Asp134 bridges the two zinc ions with one oxygen atom. In other dinuclear zinc enzymes, such as PTE, AAP, and DHO, the carboxylate group bridges by one oxygen to each zinc ion.

Finally, we note that the sulfur atom of the substrate starts to associate with Zn1. The Zn1–S distance is 2.65 Å at *Inter1*. This interaction will become important for the S–C bond cleavage step (see below).

3.3. C–S bond cleavage

Next step after the formation of *Inter1* is the C_C–S bond cleavage [23,24]. From the calculations, it turns out that a proton transfer step must take place before the C–S bond can dissociate. Every attempt to locate a transition state for the C–S bond cleavage from *Inter1* led to a transition state for a proton transfer from the μ-OH to Asp58. The optimized geometries of this transition state (called *TS2*) and the resulting intermediate (*Inter2*) are shown in Fig. 3. *TS2* has been confirmed to have one imaginary frequency of $398i\ cm^{-1}$. At *TS2*, the proton is equidistant to the two oxygen atoms (O_μ and the Asp58 oxygen) with a bond distance of 1.21 Å. With the proton delivered, the bond between O_μ and the former carbonyl carbon (C_C) is shortened from 1.52 Å to 1.45 Å, while the C_C–S bond is elongated from 1.98 Å to 2.08 Å. In addition, the distance between the sulfur atom and the Zn1 ion becomes shorter by 0.07 Å (2.65 Å vs. 2.58 Å in *Inter1* and *Inter2*, respectively). The barrier and reaction energy for this proton transfer step are calculated to be very small compared to *Inter1*, +0.3 and +0.2 kcal/mol, respectively.

At *Inter2*, the C_C–S bond is ready to break. We have located a transition state for the C–S bond cleavage from *Inter2* (*TS3*, displayed in Fig. 3). Although the barrier is calculated to be only 0.1 kcal/mol higher than *Inter2*, it is a distinct stationary point with an imaginary frequency of $79i\ cm^{-1}$. The critical C_C–S distance at *TS3* is 2.29 Å. The resulting structure, which corresponds to the enzyme–product complex (called *Prod*, see Fig. 4), is 7.5 kcal/mol lower than *Inter2* (i.e. 11.8 kcal/mol higher than *React*). It should be mentioned here that we made many attempts to locate a concerted transition state in which proton transfer from μ-OH^- takes place concomitantly with the C–S bond cleavage, but without success.

The C–S bond cleavage results in a thiolate (CH_3S^-) that coordinates to Zn1 and a lactate that coordinates to Zn2 in a bidentate fashion (see *Prod* in Fig. 3). The charge at the sulfur leads to a stronger coordination to the Zn1 ion (2.50 Å in *TS3* and 2.38 Å in *Prod*). This result indicates that the Zn1 ion plays a role in stabilizing the developing charge at the sulfur, thereby lowering the barrier for the C_C–S bond cleavage step. With the S-Zn1 bond formation, O_μ loses coordination to Zn1 (O_μ–Zn1 = 2.80 Å in *Prod*), which results in a maintained penta-coordination of Zn1 and hexa-coordination of Zn2.

3.4. Product release and active-site regeneration

At *Prod*, both products (thiolate and lactate) are negatively charged and strongly bound to their respective zinc ions (see Fig. 3). To regenerate the active site for another round of catalysis, the products have to be released and a new water molecule has to enter and form a bridging hydroxide. It is conceivable that the products are released in the charged form to the bulk solvent where they either remain unprotonated or receive a proton, depending on the acidity of the solution. To obtain exact energies of this process is very complicated and requires much larger models of the active site and also very accurate bulk solvent representation. However, from our calculations, one can make a rough estimation of the energetics involved in the ligand exchange process by using the following procedure.

First, we can estimate the energy of the overall reaction catalyzed by GlxII

$$\text{substrate} + \text{water} \rightarrow \text{methylthiol} + \text{lactic acid}$$

This can be done by calculating the energies of the individual molecules involved in the reaction (using the same computational protocol described above in Section 2). These calculations show that the overall reaction is almost thermoneutral (exothermic by 1.5 kcal/mol in the gas phase and endothermic by 0.4 kcal/mol when solvation is considered using $\varepsilon = 80$).

Since the enzyme does not change this energy, one full enzyme cycle should also be endothermic by this amount. Thus, one can estimate that the steps involved in the product release, active-site regeneration, and the binding of a new substrate to the active site, together are exothermic by ca. 11.4 kcal/mol, which is the energy of *Prod* added to the overall reaction energy (11.8–0.4 kcal/mol). Furthermore, to estimate approximately the energies involved in the individual steps, we first manually placed a water molecule in the second coordination shell of *Prod* and optimized the geometry of the complex (called *Prod-wat*, Fig. 4). Subsequently, we let this water molecule change places with either one of the two products (methylthiol and lactic acid), which now bind in their protonated forms in the second coordination shell. This ligand exchange was done manually, by changing the positions of the molecules in the model. The optimized structures of these complexes are called *Comp1* and *Comp2*, respectively (see Fig. 4). Both these structures have slightly higher energies than *Prod-wat*, *Comp1* by 0.3 kcal/mol and *Comp2* by 4.8 kcal/mol.

In the case of *Comp1* we notice that during the geometry optimization the lactate product takes a proton from the protonated Asp58 rather than from the newly-introduced water molecule (see Fig. 4). When the lactic acid is removed from the model and the geometry is re-optimized (*Comp1'*, Fig. 4) we found that the Asp58 picked up one proton of the water molecule and the resulting hydroxide became bridging the two zinc ions. To regenerate the active site, one can speculate that the thiolate might take the proton of Asp58 and get released as a neutral molecule.

Alternatively, when the methylthiol product was removed from the *Comp2* and the structure was re-optimized, something very interesting was observed. We found that the Zn1-stabilized hydroxide ($O_{Zn1}H^-$) without a barrier attacked the C_C atom of the lactate and formed a new tetrahedral intermediate (see *Comp2'* in Fig. 4). In this tetrahedral intermediate species, the O_{Zn1}–C_C distance is 1.45 Å, to be compared to the distance of 2.59 Å in *Comp2*. Simultaneously with the O_{Zn1}–C_C bond formation, a proton is delivered back from the Asp58 residue to O_μ. The O_μ–C_C bond is elongated to 1.55 Å from 1.32 Å in *Comp2*, and O_μ becomes bridging again (O_μ–Zn1 = 2.21 Å in *Comp2'*). From *Comp2'*, it is possible that the O_μ–C_C bond breaks and the active site is regenerated this way. We therefore optimized the TS for the O_μ–C_C bond cleavage and the barrier was calculated to be only 2.0 kcal/mol relative to *Comp2'* (2.5 kcal/

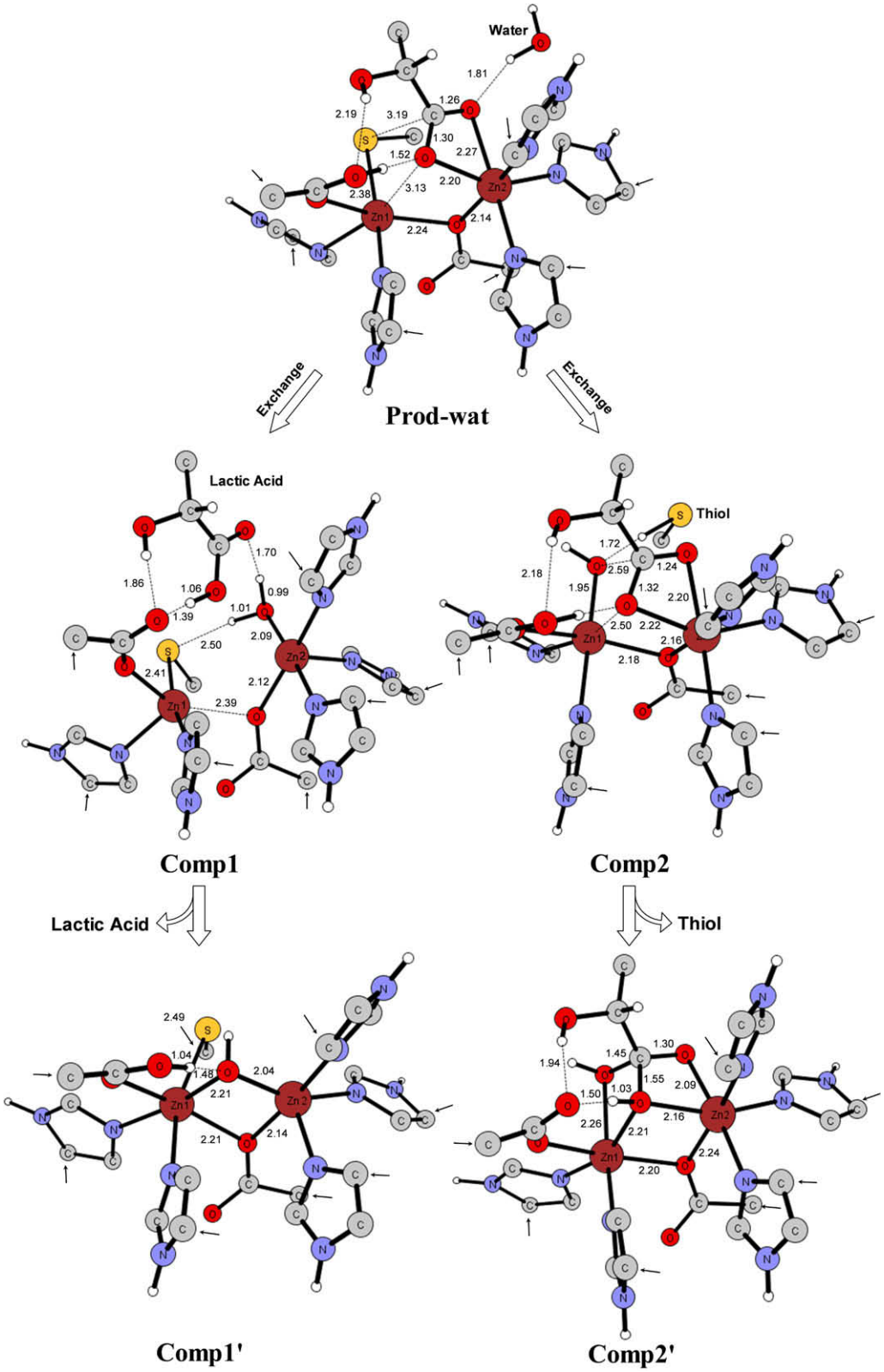

Fig. 4. Optimized structures of the complexes in the ligand exchange processes.

mol without the solvation included), indicating this step is feasible. This step, resulting in a free lactic acid and a regenerated active site, is calculated to be exothermic by 18.1 kcal/mol (17.4 kcal/mol without solvation effects). This outlined scenario for the active-site regeneration is quite novel. However, it should be stressed that it is very speculative, since it is based on quite crude estimations. These steps cannot be modeled accurately using the models and methods employed in the current study. More experimental and theoretical work will be required to make a more solid statement about the exact mechanism of active-site regeneration.

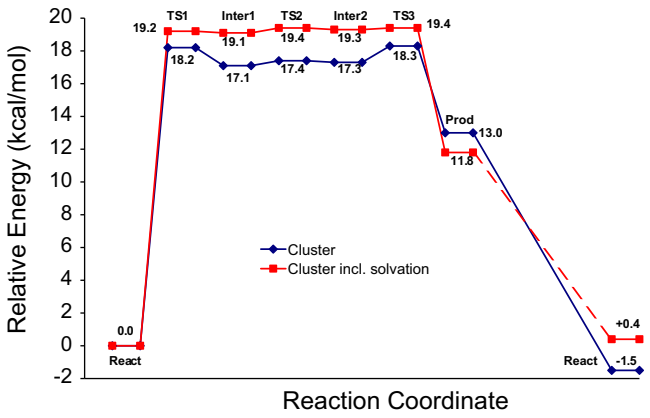

Fig. 5. Calculated potential energy profile for GlxII reaction. (Cluster) B3LYP/6-311+G(2d,2p) energies with zero-point corrections included. Solvation effects are added with dielectric constant $\varepsilon = 4$.

4. Conclusions

In this paper, we have reported a theoretical examination of the reaction mechanism of glyoxalase II. The hydrolysis of a model substrate, a small thioester formed from lactic acid and methylthiol, was investigated with an active-site model constructed on the basis of X-ray crystal structure. Transition states and intermediates along the reaction pathway were located and characterized. The optimized stationary points are shown in Figs. 2–4 and the obtained potential energy profile is presented in Fig. 5.

The calculations give general support to the previously proposed mechanism of Scheme 2 [23,24] and provides a more detailed picture of the various steps of the reaction. To summarize, the following mechanistic characteristics can be concluded from the calculations:

- Similarly to previous calculations on other dinuclear zinc enzymes, such as phosphotriesterase (PTE) [34,35], aminopeptidase from *A. proteolytica* (AAP) [37], and dihydroorotase (DHO) [46], the calculations demonstrate that the bridging hydroxide can indeed act as a nucleophile, attacking the carbonyl carbon of lactoyl group directly from its bridging position. This is an important feature that has been questioned previously [53,54].
- By studying how some important geometric parameters change during the reaction we were able to analyze the roles of the two zinc ions. Zn2 is demonstrated to stabilize the charge of the tetrahedral intermediate, lowering thereby the barrier of the nucleophilic attack. Zn1, on the other hand, stabilizes the emerging charge at the thiolate, facilitating the S–C bond cleavage step.
- The nucleophilic attack has a calculated barrier of 19.2 kcal/mol, while the later S–C bond dissociation step has a barrier of 19.4 kcal/mol. The two barriers are thus too close to make a safe conclusion from the calculations regarding which one is the rate-limiting. However, in at least three other binuclear zinc hydrolases (PTE, AAP, and DHO), calculations have shown that the initial nucleophilic attack by the bridging hydroxide is not the rate-limiting step [34,35,37,46]. It is possible that this is a general feature in binuclear zinc hydrolases. If this is the case, the results obtained for the GlxII reaction are not in contradiction with this.

It should here be mentioned that both these calculated barriers are slightly overestimated compared to the experimentally-measured k_{cat} of $2.8 \times 10^2\ s^{-1}$, which can be converted to a barrier of ca 14 kcal/mol using classical transition state theory. Several sources of error can be envisioned, such as the size of the active-site model used, the underlying theoretical method (B3LYP and the employed basis set), the homogenous solvation methods used, and the adopted coordinate locking scheme [35]. Despite this, the results of this paper provide a clear testament to the usefulness of quantum chemical active-site models to investigate mechanistic proposal of enzymes. In particular, the small difference in the potential energy profile for the cluster model with and without continuum solvation (see Fig. 5) indicates that the model, to a high degree, captures the chemistry that takes place at the enzyme active site.

Finally, the present study has also considered the steps involved in the product release and active-site regeneration. A new possible mechanism was outlined, in which the thiol product is released and replaced by a Zn-bound hydroxide. This hydroxide then attacks the lactate product, bound to the other zinc ion, to form a tetrahedral intermediate, which then collapses to yield the lactic acid and a regenerated active site with a bridging hydroxide (see Fig. 4). However, due to the limited size of the active-site model employed, the energy considerations are very crude and the conclusions of this part of the study are only speculative.

5. Abbreviations

DFT	density functional theory
GlxII	glyoxalase II
GlxI	glyoxalase I
GSH	glutathione
PTE	phosphotriesterase
AAP	aminopeptidase from *Aeromonas proteolytica*
DHO	dihydroorotase
ZPE	zero-point energies

Acknowledgments

F.H. gratefully acknowledges financial support from: The Swedish National Research Council, The Wenner-Gren Foundations, The Carl Trygger Foundation, and The Magn Bergvall Foundation. This work was also supported by grant from the Major State Basic Research Development Programs (Grant No. 2004CB719903) to W.-H.F.

References

[1] D.L. Vander Jagt, in: D. Dolphin, R. Poulson, O. Avramovic (Eds.), Coenzymes and Cofactors, vol. 3A, John Wiley and Sons, New York, 1989, pp. 597–641.
[2] B. Mannervik, in: W.B. Jakoby (Ed.), Enzymatic Basis of Detoxification, vol. 2, Academic Press, New York, 1980, pp. 263–273.
[3] P.J. Thornalley, Biochem. J. 269 (1990) 1–11.
[4] P.J. Thornalley, Mol. Aspects Med. 14 (1993) 287–371.
[5] P.J. Thornalley, Chem.-Biol. Interact. 111–112 (1998) 137–151.
[6] N. Murata-Kamiya, H. Kamiya, H. Kaji, H. Kasai, Nucleic Acids Symp. Ser. 44 (2000) 3–4.
[7] M.P. Kalapos, Toxicol. Lett. 110 (1999) 145–175.
[8] P.J. Thornalley, Gen. Pharmacol. 27 (1996) 565–573.
[9] P.J. Thornalley, M. Strath, R.J. Wilson, Biochem. Pharmacol. 47 (1994) 418–420.
[10] J.F. Bernard, D.L. Vander Jagt, J.F. Honek, Biochim. Biophys. Acta 1208 (1994) 127–135.
[11] M.J. Kavarana, E.G. Kovaleva, D.J. Creighton, M.B. Wollman, J.L. Eiseman, J. Med. Chem. 42 (1999) 221–228.
[12] R. Vince, W.B. Wadd, Biochem. Biophys. Res. Commun. 34 (1969) 593–598.
[13] D.S. Hamilton, D.J. Creighton, J. Biol. Chem. 267 (1992) 24933–24936.
[14] Y. Xu, X. Chen, J. Biol. Chem. 281 (2006) 26702–26713.
[15] J.A. Landro, E.J. Brush, J.W. Kozarich, Biochemistry 31 (1992) 6069–6077.
[16] A.D. Cameron, B. Olin, M. Ridderström, B. Mannervik, T.A. Jones, EMBO J. 16 (1997) 3386–3395.
[17] M.M. He, S.L. Clugston, J.F. Honek, B.W. Matthews, Biochemistry 39 (2000) 8719–8727.
[18] M.J. Shih, J.W. Edinger, D.J. Creighton, Eur. J. Biochem. 244 (1997) 852–857.
[19] F. Himo, P.E.M. Siegbahn, J. Am. Chem. Soc. 123 (2001) 10280–10289.

[20] M.K. Guha, D.L. Vander Jagt, D.J. Creighton, Biochemistry 27 (1988) 8818–8822.
[21] M.W. Crowder, M.K. Maiti, L. Banovic, C.A. Makaroff, FEBS Lett. 418 (1997) 351–354.
[22] J. O'Young, N. Sukdeo, J.F. Honek, Arch. Biochem. Biophys. 459 (2007) 20–26.
[23] A.D. Cameron, M. Ridderström, B. Olin, B. Mannervik, Structure 7 (1999) 1067–1078.
[24] T.M. Zang, D.A. Hollman, P.A. Crawford, M.W. Crowder, C.A. Makaroff, J. Biol. Chem. 276 (2001) 4788–4795.
[25] O. Schilling, N. Wenzel, M. Naylor, A. Vogel, M. Crowder, C. Makaroff, W. Meyer-Klaucke, Biochemistry 42 (2003) 11777–11786.
[26] N.F. Wenzel, A.L. Carenbauer, M.P. Pfiester, O. Schilling, W. Meyer-Klaucke, C.A. Makaroff, M.W. Crowder, J. Biol. Inorg. Chem. 9 (2004) 429–438.
[27] G.P.K. Marasinghe, I.M. Sander, B. Bennett, G. Periyannan, K.-W. Yang, C.A. Makaroff, M.W. Crowder, J. Biol. Chem. 280 (2005) 40668–40675.
[28] V.A. Campos-Bermudez, N.R. Leite, R. Krog, A.J. Costa-Filho, F.C. Soncini, G. Oliva, A.J. Vila, Biochemistry 46 (2007) 11069–11079.
[29] M.S. Silva, L. Barata, A.E. Ferreira, S. Romao, A.M. Tomas, A.P. Freire, C. Cordeiro, Biochemistry 47 (2008) 195–204.
[30] S. Melino, C. Capo, B. Dragani, A. Aceto, R. Petruzzelli, Trends Biochem. Sci. 23 (1998) 381–382.
[31] N.O. Concha, B.A. Rasmussen, K. Bush, O. Herzberg, Structure 4 (1996) 823–836.
[32] H. Park, E.N. Brothers, K.M. Merz Jr., J. Am. Chem. Soc. 127 (2005) 4232–4241.
[33] S.D. Aubert, Y.C. Li, F.M. Raushel, Biochemistry 43 (2004) 5707–5715.
[34] S.-L. Chen, W.-H. Fang, F. Himo, J. Phys. Chem. B 111 (2007) 1253–1255.
[35] S.-L. Chen, W.-H. Fang, F. Himo, Theor. Chem. Acc. 120 (2008) 515–522.
[36] W. Desmarais, D. Bienvenue, K.P. Bzymek, G.A. Petsko, D. Ringe, R.C. Holz, J. Biol. Inorg. Chem. 11 (2006) 398–408.
[37] S.-L. Chen, T. Marino, W.-H. Fang, N. Russo, F. Himo, J. Phys. Chem. B 112 (2008) 2494–2500.
[38] F. Himo, P.E.M. Siegbahn, Chem. Rev. 103 (2003) 2421–2456.
[39] P.E.M. Siegbahn, Q. Rev. Biophys. 36 (2003) 91–145.
[40] L. Noodleman, T. Lovell, W.-G. Han, J. Li, F. Himo, Chem. Rev. 104 (2004) 459–508.
[41] P.E.M. Siegbahn, T. Borowski, Acc. Chem. Res. 39 (2006) 729–738.
[42] F. Himo, Theor. Chem. Acc. 116 (2006) 232–240.
[43] A.D. Becke, J. Chem. Phys. 98 (1993) 1372–1377.
[44] A.D. Becke, J. Chem. Phys. 98 (1993) 5648–5652.
[45] C. Lee, W. Yang, P.G. Parr, Phys. Rev. B: Condens. Matter Mater. Phys. 37 (1988) 785–789.
[46] R.-Z. Liao, J.-G. Yu, F.M. Raushel, F. Himo, Chem. Eur. J. 14 (2008) 4287–4292.
[47] V. Barone, M. Cossi, J. Phys. Chem. A 102 (1998) 1995–2001.
[48] R. Cammi, B. Mennucci, J. Tomasi, J. Phys. Chem. A 103 (1999) 9100–9108.
[49] A. Klamt, G. Schüürmann, J. Chem. Soc., Perkin. Trans. 2 (1993) 799–805.
[50] J. Tomasi, B. Mennucci, R. Cammi, Chem. Rev. 105 (2005) 2999–3093.
[51] R. Sevastik, F. Himo, Bioorg. Chem. 35 (2007) 444–457.
[52] M.J. Frisch et al., Gaussian 03, Revision D.01, Gaussian Inc., Wallingford, CT, 2004.
[53] N.V. Kaminskaia, C. He, S. Lippard, Inorg. Chem. 39 (2000) 3365–3373.
[54] C. Jackson, H.-K. Kim, P.D. Carr, J.-W. Liu, D.L. Ollis, Biochim. Biophys. Acta 1752 (2005) 56–64.